Title

Rates of Ligand Exchange around the Bis-Oxalato Complex [NpO2(C2O4)2]3− Measured by Using Multinuclear NMR Spectroscopy under Neutral to Semi-Alkaline Conditions

Journal

ChemPlusChem, 83(7)

ISSN

0010-0765

Authors

Pilgrim, Corey D
Mason, Harris E
Zavarin, Mavrik
et al.

Publication Date

2018-07-01

DOI

10.1002/cplu.201800025

Peer reviewed

Rates of ligand exchange around the bis-oxalato complex $NpO_2(C_2O_4)_2^{3-}$ measured using multinuclear NMR at neutral to semi-alkaline conditions

Corey D. Pilgrim, [a] Harris E. Mason, [b] Mavrik Zavarin, [b] and William H. Casey*[a]

Dedication I leave this to you, Bill.

Abstract: The kinetics of ligand exchange of free oxalate, $C_2O_4^{2-}$, with the bis-oxalato Np(V) complex, $NpO_2(C_2O_4)_2^{3-}$, in aqueous solution are reported using ^{13}C and ^{17}O nuclear magnetic resonance (NMR) methods. Rates of exchange are measured in the pH regime of 6.5 – 9.0, where the speciation is shown to be stable. As the complex is paramagnetic, rates of exchange are estimated by following the width of the ^{13}C peak and ^{17}O peak assigned to the free oxalate in solution and by applying the Swift-Connick method for measuring rates of exchanges. A set of experiments where pH and total oxalate concentration are varied was run, and the linear dependence of the rate on these parameters is analyzed. Variable-temperature NMR was also run to measure activation parameters of the complexation. At pH < 8.0, $\Delta H^{\ddagger}$ = 17.5 ± 6.1 kJ·mol^{-1} and $\Delta S^{\ddagger}$ = -114 ± 21.1 kJ·mol^{-1}·K^{-1}, while at pH >8.0 there is almost no linear dependence on temperature.

Introduction

Spent nuclear fuel and radioactive waste will likely be stored in geologic media.[1–4] As such, one of the most pressing concerns in environmental chemistry is establishing a robust understanding of the aqueous transport of actinides in the shallow Earth.[5] Of the radioactive elements in waste, one of the longest-lived is ^{237}Np, which has a half-live of 2.14 million years.[6] The chemistry of this element has been explored since its discovery in 1939,[7] but is environmentally complex because of the many different oxidation states available to it.[8] Experiments are also difficult to run due to its natural radioactivity. The available oxidation states range from +3 to +7, with the most stable form in oxic environments being Np(V), where the central neptunium is tightly bound to two axial oxygens in the "-yl" moiety, making the neptunyl ion, NpO_2^+.[8,9]

Oxalate is a natural chelating ligand[10] and forms 1:1 and 1:2 complexes with NpO_2^+ with stability constants of: $\log\beta_1$ = 3.9 ± 0.1 and $\log\beta_2$ = 5.8 ± 0.2, corresponding to the reactions:[11]

$$NpO_2^+{}_{(aq)} + C_2O_4^{2-}{}_{(aq)} \leftrightarrow NpO_2(C_2O_4)^-{}_{(aq)} \quad \text{(Equation 1)}$$

and:

$$NpO_2^+{}_{(aq)} + 2C_2O_4^{2-}{}_{(aq)} \leftrightarrow NpO_2(C_2O_4)_2^{3-}{}_{(aq)} \quad \text{(Equation 2)}$$

Herein we report kinetic parameters of the self-exchange of oxalate around the bis-oxalato $NpO_2(C_2O_4)_2^{3-}$ complex using both ^{13}C NMR and ^{17}O NMR. The studied reaction is:

$$NpO_2(C_2O_4)_2^{3-}{}_{(aq)} + {}^*C_2O_4^{2-}{}_{(aq)} \leftrightarrow NpO_2(C_2O_4)({}^*C_2O_4)^{3-}{}_{(aq)} + C_2O_4^{2-}{}_{(aq)} \quad \text{(Equation 3)}$$

where the marked oxalate helps to highlight the self-exchange reaction. This ligand-exchange reaction is important both technologically and geochemically, as oxalate is the conjugate base of one of the simplest acids found in soils, where it is a product of fungal metabolism, and it is also used in the PUREX process for purifying uranium and plutonium.[12–14] Self-exchange reactions provide a good test case for computer-based predictive models of coordination chemistry since there is no net change in Gibbs' Free Energy. In Equation 6.3, the reactants and products are identical. This research complements the existing work on homoleptic water-exchange reactions for transition metals[15–20] and studies of the carbonato complexes of other transuranics.[21–24]

Results and Discussion

Initial Experiments: The complexation of the oxalate anion to the solvated NpO_2^+ was followed using UV/Vis spectroscopy, which qualitatively matched those spectra produced by Rao, *et al.*[25] where the maximum absorbance of the bare neptunyl ion at 980 nm shifted to a new maximum of absorbance at 995 nm, which corresponds to the bis-oxalato complex. However, a shoulder was seen in every spectrum centered at 987 nm, which indicates a minor amount of the mono-oxalato complex is also present in solution (Figure 1).

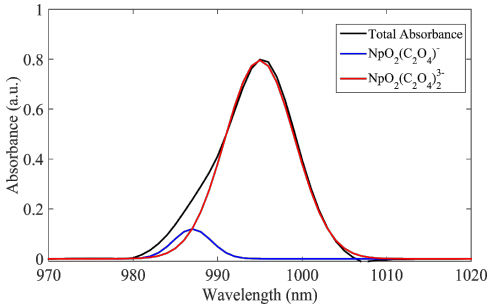

Figure 1. A representative absorbance spectrum of the mixture of $NpO_2(C_2O_4)^-$ and $NpO_2(C_2O_4)^{3-}$ in aqueous solution, with no free NpO_2^+ seen.

[a] C.D. Pilgrim, Prof. Dr. W.H. Casey
Department of Chemistry
University of California, Davis
1 Shields Ave., Davis, CA, USA 95616
E-mail: whcasey@ucdavis.edu

[b] Dr. H.E. Mason, Dr. M. Zavarin
Glenn T. Seaborg Institute, Physical and Life Sciences Directorate
Lawrence Livermore National Laboratory
7000 East Avenue, Livermore, CA, USA 94550

Supporting information for this article is given via a link at the end of the document.

A solution was made in order to follow the absorbance peaks seen in the UV/Vis spectrum with pH varying from 5 to 9, to see if this change had any effect on the overall $[NpO_2(C_2O_4)^-]/[NpO_2(C_2O_4)_2^{3-}]$ ratio. As expected from the speciation calculations, there was no observed shift in the ratio across this pH range.

Curiously, while the UV/Vis spectra showed the presence of both the $NpO_2(C_2O_4)^-$ and $NpO_2(C_2O_4)_2^{3-}$ complexes, the ^{13}C NMR spectrum has only two singlets. After comparison to a solution containing only ^{13}C-labeled oxalate, one peak arises from the excess oxalate in solution, where the chemical shift lies between 167 and 170 ppm, depending on the pH of the solution. The second singlet (between 1 and 3 ppm) must be due to a bound oxalate species, but only one peak is seen when two are expected. A representative ^{13}C spectrum is included in Figure 2.

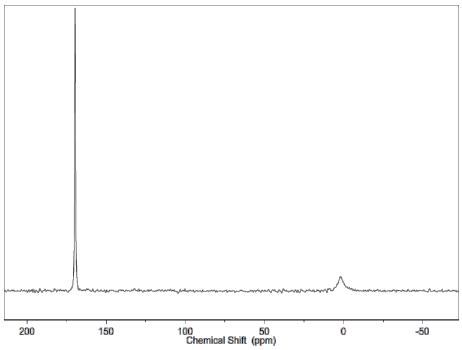

Figure 2. ^{13}C NMR spectrum of a solution containing excess ^{13}C-labeled oxalate. Note that the downfield peak is due to excess oxalate in solution.

In all ^{13}C NMR experiments, only one peak for the complexed species was observed in the spectrum, even during the variable-temperature experiments. In cases where the solutions were made with ^{17}O-labeled oxalic acid, ^{17}O NMR showed only a broad peak at around 264 ppm. After comparison to a solution of only ^{17}O-labeled oxalic acid, this peak is assigned to the free oxalate ion in solution, while the bound oxalate is not observed because the coordinated oxygens would be in direct contact with the paramagnetic Np(V), which would broaden the signal into the baseline.

One sample was created to try to measure the mono-oxalato species in solution (Solution A), where a minimum of oxalate was added to the solution. Only a single peak in the ^{13}C NMR spectrum was seen with this sample, which was found around -1 ppm. With this, it has been surmised that the peak that is seen in all other samples (where $[C_2O_4^{2-}]_{total} > [NpO_2^+]$) that is attributed to the bound oxalate is a mixture of the two species, as the overlap between the peaks (due to the broadness of the peaks and any exchange between the two species) makes it impossible to separate out. Thus, only exchange between the observed signal and the free oxalate can be measured, which will be the best approximation available.

Swift-Connick Methodology: The Swift-Connick method of analysis was used for rate determination with both the ^{13}C and ^{17}O-labeled samples.[21,26] To understand the Swift-Connick formalism, one must understand what determines the peak-width of an NMR signal. The full-width at half-maximum (FWHM) of an NMR signal, when measured for a peak in a system undergoing two-site exchange, is generally defined as:

$$\pi(FWHM) = 1/T_2^* + k_{ex} \quad \text{(Equation 4)}$$

where T_2^* is the transverse relaxation time with magnetic inhomogeneity effects included, and k_{ex} k_{ex} is the rate coefficient for the observed exchange process, either for the bound peak ($k_{ex,b}$) or the free peak ($k_{ex,f}$). Generally, $k_{ex,b}$ is reported in the literature for these exchange reactions. However, when only the free peak is seen in an NMR spectrum, one must invoke the Swift-Connick formalism, which utilizes the Law of Detailed Balance:

$$k_{ex,b}X_b = k_{ex,f}X_f \; k_{ex,b}X_b = k_{ex,f}X_f \quad \text{(Equation 5)}$$

where X is the mole fraction of either the bound (b) or free (f) species. At the slow-exchange limit (where the measured peaks continue to broaden with increased temperature), the Swift-Connick formalism describes the full-width at half-max of the 'free' peak as:[27]

$$\pi(FWHM_p\text{-}FWHM_n) = k_{ex,f} = k_{ex,b}X_b/X_f \quad \text{(Equation 6)}$$

The subscript on the FWHM term denote the measured peak width in the present of a paramagnet (p) or without the paramagnet in solution (n). The $FWHM_n$ term in Eq. 6 accounts for the natural linewidth ($1/T_2^*$) term from Eq. 4, as there should be no exchange reaction occurring without the paramagnet in solution. To measure $FWHM_n$, a ^{17}O-labeled or ^{13}C-labeled oxalate solution was prepared at the pH of each original solution. Thus, all reported bound rates of exchange are calculated from changes in the NMR spectrum assigned to the unbound (free) ligand in solution

Rate Dependence on pH and Oxalate Concentration through ^{13}C NMR: A series of five solutions of differing ^{13}C-labeled oxalate concentration were made from the same dilution of the original neptunium stock ($[NpO_2^+]$ = 5.1 mM), with $[C_2O_4^{2-}]_{total}$ for these solutions ranging from 4.4 mM to 108.1 mM. The lowest value of $[C_2O_4^{2-}]_{total}$ allowed samples to include a solution with barely enough oxalate to fully complex the free neptunium in a 1:1 ratio, to help interpret the initial ^{13}C NMR spectra, where only a single bound peak was observed. These five solutions were set to an initial pH = 6.5 ± 0.03, and UV/Vis and ^{13}C NMR spectra were collected for each sample. This was repeated a total of seven times to encompass the pH range of 6.5 to 9.0. Table 1 compiles the different initial solution parameters, and also compiles the measured molarities of the constituents after deconvolution of the UV/Vis spectra, as per the absorbance parameters reported in Rao, *et al*.[25]

Table 1. Initial solution parameters (at pH 6.5) of Variable pH/variable $[C_2O_4^-]$ samples

Solution ID	$[C_2O_4^{2-}]_{total}$, mM	$[NpO_2^+]$, mM[a]	$[NpO_2(C_2O_4)^-]$, mM[a]	$[NpO_2(C_2O_4)^{3-}]$, mM[a]
A	4.4	0.6	3.4	1.0
B	16.2	0.1	2.0	3.1
C	40.4	0.09	0.7	4.2
D	78.0	0.05	0.4	4.8
E	108.1	0.04	0.4	4.7

[a] Measured using the UV/Vis spectra at pH = 6.5, where ε_a = 395 $M^{-1}cm^{-1}$ for NpO_2^+, 391 $M^{-1}cm^{-1}$ for $NpO_2(C_2O_4)^-$, and 382 $M^{-1}cm^{-1}$ for $NpO_2(C_2O_4)^{3-}$.

As expected, when excess oxalate is added to the system, the bis-oxalato species dominates the speciation. As the pH is increased, the amount of oxalate in does solution seems to affect the absolute amounts of the constituent species in solution, where the two samples with lower $[C_2O_4^{2-}]_{total}$ are affected much more strongly, which is shown in Figure 3.

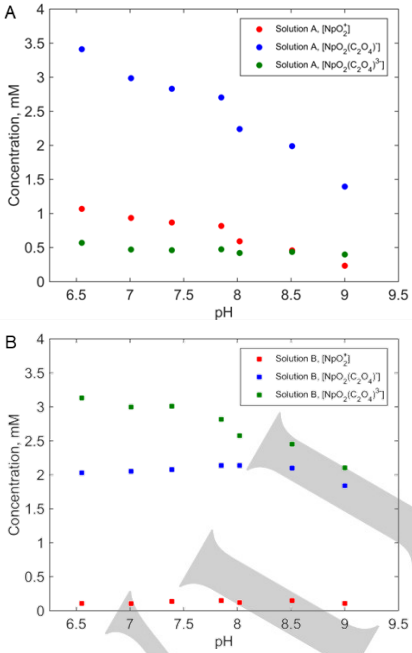

Figure 3. Plots showing the variation in the concentrations of solution constituents versus pH for Solutions A and B, which have the two lowest $[C_2O_4^{2-}]_{total}$.

This drop in dissolved neptunium was also visible to the naked eye, as at higher pH values, Solutions A and B began to get cloudy. The UV/Vis absorbance dropped substantially (in the case of Solution A, by 60%), due to the loss of dissolved neptunium that is most likely occurring as the hydroxide complexation is outcompeting the oxalate complexation. This effect could cause mixed-hydroxide/oxalate complexes form and settle out from solution. At the higher oxalate concentrations, this is much less pronounced, probably due to the higher availability of oxalate, where the UV/Vis absorbance is decreasing due to the dilution caused as a side effect of changing the pH.

The free oxalate peak observed in the ^{13}C NMR of these five samples substantially broadened when the pH was increased through the entire pH range. Using the Swift-Connick methodology discussed earlier, the calculated $k_{ex,b}$ also followed this trend. Only Solutions C-E are useful in this analysis, as one of the requirements of the analysis is having a dependable free oxalate peak, which is not found in Solutions A and B because of the low $[C_2O_4^{2-}]_{total}$. As seen in Figure 4, the increase in exchange rate is nearly the same between the three higher $[C_2O_4^{2-}]_{total}$ values, with the average of the slopes of the best-fit lines being 0.46 ± 0.02.

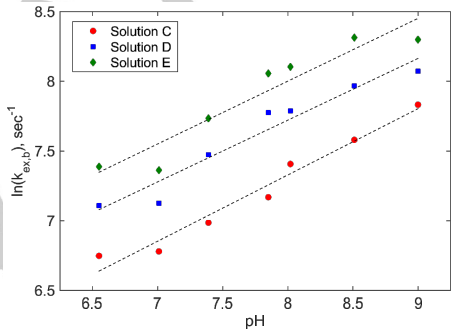

Figure 4. Plot of the natural log of the rate coefficient, $k_{ex,b}$, versus pH for Solutions C-E. Best-fit lines for each of the series are included as the dotted lines.

This dependence on exchange rate with pH can be explained when knowing the structure of the complex in solution. Neptunyl ions can complex either five or six oxygens in the equatorial plane, depending on the ligand present.[31-33] Of these six possible sites, four are taken up by the two sets of oxygens on the bidentate oxalate ligands in the neptunyl-oxalate complexes. Due to the size of the oxalate ligand, only five equatorial positions are open, and the last site adopts water as a ligand. At solution pH ≥ 9.0, it has been observed that mixed hydroxide/oxalate species can form.[11,34] Thus, we hypothesize that as the pH is increased in this system, the bound water can hydrolyze to form a bound hydroxide, which increases the rate of exchange of the bound oxalate (Figure 5). The added electron density that this hydroxyl donates to the neptunyl center then allows the remaining oxalate ligands to become more labile and more open to exchange.

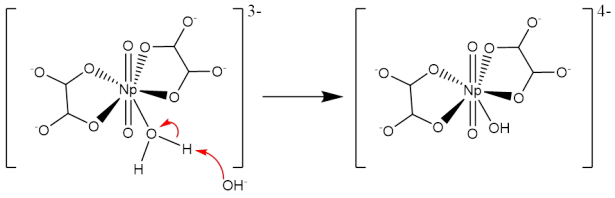

Figure 5. Proposed hydrolysis scheme of $NpO_2(C_2O_4)_2(H_2O)^{3-}$ at alkaline pH.

The measured rates of exchange were also compared between the samples with differing concentrations of unbound oxalate in solution ($[C_2O_4^{2-}]_{free}$), with the pH held constant. When doing this, an increase in $k_{ex,b}$ was observed to be concomitant with increasing $[C_2O_4^{2-}]_{free}$. In the case of the graph, the natural logarithm of $k_{ex,b}$ was plotted against the natural logarithm of $[C_2O_4^{2-}]_{free}$, to try to understand the rate order of the process. This is shown for each of the seven pH values (Figure 6), where again, Solutions C-E are analyzed. However, the slopes of the lines jumped between 0.39 and 0.78, though the same increasing trend is seen in each set of data. We believe this variation gives a reasonable error to this trend, such that the average value of the slope is 0.58 ± 0.12.

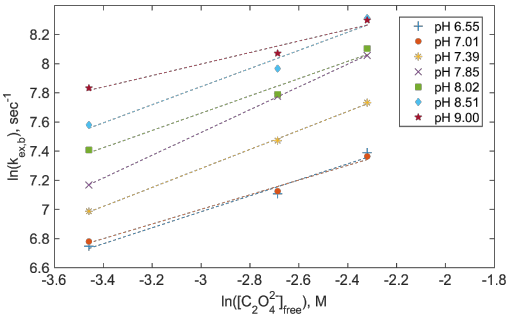

Figure 6. Variation of $k_{ex,b}$ with increasing $[C_2O_4^{2-}]_{free}$. Each set of samples (from Solutions C-E) were held at a constant pH.

Variable-Temperature NMR: Another set of solutions containing either ^{13}C- or ^{17}O- labeled oxalaate were created from the neptunium stock solution. These solutions where used for variable-temperature NMR (VT-NMR) measurements. The pH range was chosen once again create conditions where the bis-oxalato complex dominates the speciation (pH 6.5 -9), with concentrations and pH as specified in Table 2.

Table 2. Solution conditions for VT-NMR experiments with both ^{13}C- and ^{17}O-labeled oxalate solutions.

Solution ID	pH	$[NpO_2^+]_{total}$, mM[a]	$[C_2O_4^{2-}]_{total}$, mM[b]	X_f[c]
1	*7.44*	*3.5*	*43.6*	*0.913*
2	7.56	4.4	41.2	0.881
3	*7.71*	*2.4*	*50.3*	*0.950*
4a	7.70	4.7	29.0	0.808
4b	7.77	5.1	42.5	0.863
4c	7.86	5.2	53.5	0.893
5	8.30	3.4	72.7	0.950
6	8.98	4.4	41.7	0.883

Italics designate solutions made with ^{17}O-labeled oxalate. [a] Calculated using UV/Vis spectra taken when solution was made. [b] Measured gravimetrically. [c]X_b omitted, as 1- X_f = X_b

These samples were subjected to VT-NMR, where the temperatures ranged from 298K to 338K in 5K steps, which is an order of magnitude larger than the experimental uncertainty of ± 0.5K. The lineshape of each signal broadened as the temperature increased, but complete coalescence in the ^{13}C spectra was not observed as the large difference in chemical shift between the two species ($\Delta\omega$ = 24,000 Hz) made it impossible to observe. An example of a variable temperature experiment using ^{13}C-labeled oxalate can be seen in Figure 7.

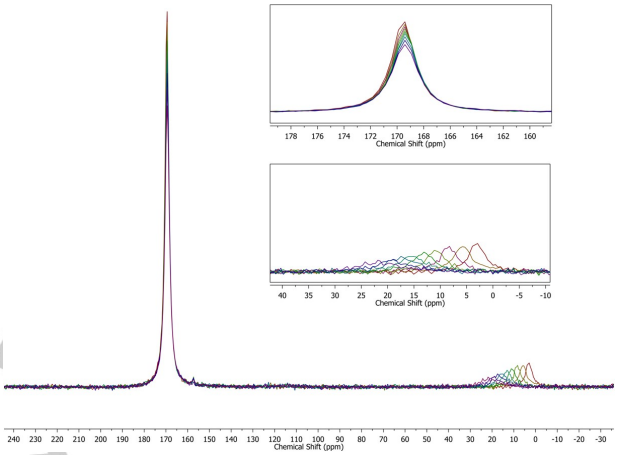

Figure 7. Variable temperature ^{13}C NMR of Solution 5 (pH 8.30). Each color represents a single temperature measurement. Top insert: The signal due to free oxalate. Bottom insert: Bound oxalate. The minor peak at 157 ppm was due to an impurity and was not included in the analysis as it did not exhibit broadening due to variable temperature.

Solutions of ^{13}C-labeled oxalate and ^{17}O-labeled oxalic acid were measured using VT-NMR absent of the neptunyl ion to account for the natural linewidth of the species in solution. For the ^{13}C oxalate, the natural linewidth relatively constant with increased temperature (it broadened from 1.1 to 1.5 Hz). For the ^{17}O oxalic acid, no variation of the natural linewidth observed with changing pH, but there was temperature-induced sharpening of the peak (164 to 82 Hz), which was expected due to the decreased viscosity (and correlation time, τ_c) at higher temperature, which leads to higher T_2 values for this quadrupolar nucleus.[28]

An Eyring analysis was conducted on all VT-NMR results, where the Eyring-Polanyi equation was used to determine activation parameters of the exchange:

$$\ln(k_{ex,b}/T) = \ln(k_b/h)(-\Delta G^{\ddagger}/RT) \qquad \text{(Equation 7)}$$

where k_b is the Boltzmann constant, h is Planck's constant, R is the gas constant, $\Delta G^{\ddagger}$ is Gibbs energy of activation, and T is temperature.[29,30] Graphically, $\ln(k_{ex,b}/T)$ for the bound oxalate peak is plotted versus 1/T in Figure 8 and a linear regression is applied to the data sets. The activation parameters extracted from this regression are compiled in Table 3. For the solutions at pH < 8.0, there is a clear trend observed in the rate of exchange of the bound oxalate. However, at pH > 8.0, the slope of this trend levels to near zero and the rate of exchange of the bound

oxalate has almost no dependence on temperature. Also, through the course of these experiments, the ^{17}O NMR data contains slightly higher activation parameters than the ^{13}C NMR data. The activation parameters for solutions 5 and 6 are quite different than the rest, due to the insensitivity the rate of exchange shows to temperature at those pHs.

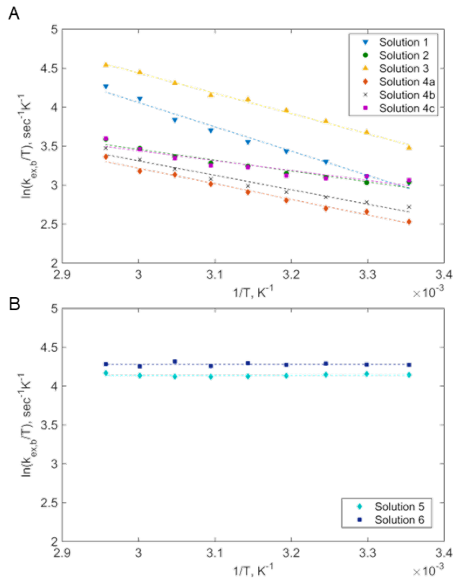

Figure 8. Eyring plots for all VT-NMR experiments, with all solutions defined in Table 2. **A:** All solutions (including ^{13}C and ^{17}O) where pH < 8. **B:** For the two solutions above pH 8.0

Table 3. Compiled activation parameters from the Eyring analysis.

Solution ID	pH	$\Delta H^{\ddagger}$, kJ/mol	$\Delta S^{\ddagger}$, J/(molK)
1	*7.44*	*27.4*	*-81.6*
2	7.56	13.8	-127.3
3	*7.71*	*21.6*	*-95.7*
4a	7.70	16.6	-120.9
4b	7.77	15.4	-137.9
4c	7.86	10.4	-120.9
5	8.30	-0.030	-163.0
6	8.98	-0.103	-162.3

Italics again designate the solutions made using ^{17}O-labeled oxalate.

As can be seen in Figure 8 and Table 2, at pH < 8.0 there is a similarity in the Eyring curves and subsequent activation data for all samples measured. When the ^{13}C and ^{17}O data are treated separately, the activation parameters calculated from the ^{13}C VT-NMR are $\Delta H^{\ddagger}$ = 14.1 ± 2.7 kJ/mol with $\Delta S^{\ddagger}$ = -127.5 ± 7.4 J/(mol·K), while the activation parameters from the ^{17}O VT-NMR are calculated to be $\Delta H^{\ddagger}$ = 24.5 ± 4.1 kJ/mol with $\Delta S^{\ddagger}$ = -88.7 ± 10.0 J/(mol·K). The difference between these two methods provides a good estimate for error in these calculations. Thus, reported values for the activation parameters are the combined averages between the two data sets: $\Delta H^{\ddagger}$ = 17.5 ± 6.1 kJ/mol and $\Delta S^{\ddagger}$ = -114.1 ± 21.1 J/(mol·K). This calculated activation enthalpy is relatively low when compared to the values measured for water exchange around the transition metals, but not entirely uncommon.[15] The lowered energy barrier for the exchange is likely due to the presence of the spectator water ligand, which also is sensitive to pH and helps to labilize the bound oxalates.[16]

Conclusions

^{13}C and ^{17}O NMR show that the mixture of stable $NpO_2(C_2O_4)^-$ and $NpO_2(C_2O_4)_2^{3-}$ complex undergoes rapid exchange with free oxalate in aqueous solution. The speciation of this system is dominated by the bis-oxalato species at high oxalate concentration, and this speciation does not change with pH when there is excess oxalate in the system. The exchange rate of this self-exchange depends on both the pH of the solution and the concentration of the free oxalate. Eyring analysis of the line-broadening due to exchange indicates a relatively low value for activation enthalpy ($\Delta H^{\ddagger}$ = 17.5 ± 6.1 kJ/mol) and a moderately negative activation entropy ($\Delta S^{\ddagger}$ = -114.1 ± 21.1 J/(mol·K)).

Experimental Section

Caution! Neptunium-237 is an alpha (α) emitter that is potentially harmful. Extreme care must be taken when using this material. It should be handled at a dedicated facility with the proper engineering controls.

Solution Preparation: A stock solution of dissolved Np(V) was prepared as described previously, though no $KBrO_3$ was added, as the +5 oxidation state was the desired state for complexation with oxalate.[24] ^{13}C-labeled $Na_2C_2O_4$ was used as received from Sigma-Aldrich (99% $^{13}C_2$) with no purification. ^{17}O-labeled $H_2C_2O_4$ was prepared using 0.092 g of unlabeled $Na_2C_2O_4$ (Sigma-Aldrich), which was dissolved in 2 mL ^{17}O-labeled H_2O (35-40%, Cambridge Isotope Labs). To ensure complete exchange with ^{17}O-labeled H_2O, The pH of this solution was adjusted to pH = 2.5 using concentrated HCl and was then capped and placed in an oil bath at 80°C overnight.[35,36] The water was evaporated off using a vacuum pump and the remaining solid was washed with ethanol to remove any remaining acid. After drying, 0.054g of solid $H_2C_2O_4$ was obtained. ^{17}O NMR was used to confirm the presence of the ^{17}O-label in the oxalate.

Aliquots of the 10 mM Np(V) stock solution were diluted to create solutions with metal concentration between 2.0 and 5.2 mM. Solid ^{13}C-labeled $Na_2C_2O_4$ or solid ^{17}O-labeled $H_2C_2O_4$ were added to these solutions to reach ligand concentrations between 5 and 100 mM. Solutions were made in D_2O (99.5%, Cambridge Isotope Labs) for the purpose of providing a lock solvent for the NMR spectrometers. The pH was adjusted using dilute solutions of NaOH and HNO_3, and was

measured via a calibrated Metrohm Biotrode™ microelectrode. `

Complexation of Np(V) by oxalate can be followed via UV/Vis spectrophotometry, where quantification of the solution concentration/speciation was obtained by using absorbance wavelengths and molar absorptivities published by Rao et al.[25] A Cary 6000i spectrophotometer (Agilent) was used with 1.0 cm microcuvettes that limited the volume needed to 0.5 mL. The subsequent spectra were fit and deconvoluted using Matlab® to provide accurate concentrations of the constituents.

NMR Parameters: Solutions were placed in 5 mm PTFE-FEP NMR liners (Wilmad) and then glass NMR tubes, in order to provide two barriers to prevent contamination of the spectrometer in the unlikely event of a broken tube. Spectra were measured using a 14.1 T magnet (150.8 MHz for ^{13}C, 81.4 MHz ^{17}O) coupled to a Bruker Avance III console with a 5 mm PABBO probe for solutions. The recycle delay was set to 0.5 s for all measurements, as the presence of the paramagnetic Np(V) caused the measured T_1 values to be ≤ 1.5 ms. The pulse times were calibrated at 95W for the ^{13}C measurements (π/2 = 9.5 μs) and at 110W for the ^{17}O measurements (π/2 = 13 μs). A one-dimensional T_1-inversion recovery pulse program (with inversion delay = 0.3 sec) was used for all ^{13}C measurements to filter out the background from the Teflon liners, as the T_1 values for the solution and solid liner were vastly different. No diminishment of the peaks of interest was seen when compared to a simple 1D spectrum. A previous temperature calibration for the probe was used, but was checked against the chemical shifts of d_4-methanol using the 'calctemp' protocol in the TopSpin® software and temperatures deviated < 0.5°C, so the raw temperatures are used in all subsequent analysis. Spectra were fit using MestReNova® to provide linewidth and chemical shift.

Speciation Calculations: Speciation calculations for a solution consisting of 3 mM total dissolved Np(V) was modeled with an excess of total dissolved oxalate (53 mM) as a function of pH, to mimic the experimental conditions. The Davies model for activity correction was used in these calculations.[37] These calculations were performed using Visual MINTEQ with the included thermodynamic database.[38] This database included the stability constants for the formation of the mono- and bis-oxalato complexes, found in Ref. 11. In the simulation, there is no change in speciation when between pH 6.5 and 12, with the predominant neptunium species in solution being the bis-oxalato complex, $NpO_2(C_2O_4)_2^{3-}$, at roughly 88% of total dissolved neptunium by concentration. The minor species is the mono-oxalato complex, $NpO_2(C_2O_4)^-$, at the remaining 12%. Calculated speciation diagrams are included in the Supporting Information.

Acknowledgements

This work was supported by the Office of Basic Energy Science of the U.S. Department of Energy as part of the Materials Science of Actinides Energy Frontier Research Center (DE-SC0001089) to W.H.C. The work at LLNL was supported by the Subsurface Biogeochemical Research Program of the U.S. Department of Energy'sOffice of Biological and Environmental Research under Contract DE-AC52- 07NA27344 to LLNL. C.D.P. was supported by a graduate student fellowship from Department of Energy via the Nuclear Energy University Program-Integrated University Program.

Conflict of Interest

The authors declare no conflict of interest.

Keywords: Neptunium • ^{13}C-NMR • Complexation Chemistry • Kinetics Variable-temperature NMR

[1] G. R. Choppin, *Mar. Chem.* **2006**, *99*, 83–92.
[2] A. B. Kersting, *Inorg. Chem.* **2013**, *52*, 3533–3546.
[3] P. Zhao, R. M. Tinnacher, M. Zavarin, A. B. Kersting, *J. Environ. Radioact.* **2014**, *137*, 163–172.
[4] W. Runde, M. P. Neu, in *The Chemistry of the Actinides and Transactinide Elements* (Eds.: L. Morss, N. Edelstein, J. Fuger), Springer, **2010**, pp. 3475–3593.
[5] M. I. Ojovan, W. E. Lee, in *An Introduction to Nuclear. Waste Immobilization*, Elsevier, **2014**.
[6] F. P. Brauer, R. W. Stromatt, J. D. Ludwick, F. P. Roberts, W. L. Lyon, *J. Inorg. Nucl. Chem.* **1960**, *12*, 234–235.
[7] E. McMillan, P. H. Abelson, *Phys. Rev.* **1940**, *57*, 1185–1186.
[8] Z. Yoshida, S. G. Johnson, T. Kimura, J. R. Krsul, in *The Chemistry of the Actinides and Transactinide Elements* (Eds.: L. Morss, N. Edelstein, J. Fuger), **2010**, pp. 699–812.
[9] J. C. Eisenstein, M. H. L. Pryce, *Proc. R. Soc. A Math. Phys. Eng. Sci.* **1955**, *229*, 20–38.
[10] G. R. Choppin, M. P. Jensen, in *The Chemistry of the Actinides and Transactinide Elements* (Eds.: L. Morss, N. Edelstein, J. Fuger), **2010**, pp. 2524–2621.
[11] W. Hummel, G. Anderegg, L. Rao, I. Puigdomènech, O. Tochiyama, *Chemical Thermodynamics of Compounds and Complexes of U, Np, Pu, Am, Tc, Se, Ni and Zr with Selected Organic Ligands*, **2005**.
[12] W. C. Graustein, K. Cromack, P. Sollins, *Science* **1977**, *198*, 1252–4.
[13] N. Vigier, S. Grandjean, B. Arab-Chapelet, F. Abraham, *J. Alloys Compd.* **2007**, *444–445*, 594–597.
[14] D. O. Campbell, S. R. Buxton, *Recovery of Transplutonium Elements from Nuclear Reactor Waste*, **1977**, 4,025,602.
[15] L. Helm, A. E. Merbach, *Coord. Chem. Rev.* **1999**, *187*, 151–181.
[16] L. Helm, A. E. Merbach, *Chem. Rev.* **2005**, *105*, 1923–1960.
[17] I. Farkas, I. Banyai, Z. Szabo, U. Wahlgren, I. Grenthe, *Inorg. Chem.* **2000**, *39*, 799–805.
[18] I. Farkas, I. Grenthe, *J. Phys. Chem. A* **2000**, *104*, 1201–1206.
[19] Z. Szabo, J. Glaser, I. Grenthe, *Inorg. Chem.* **1996**, *35*, 2036–2044.
[20] W. Aas, Z. Szabó, I. Grenthe, *J. Chem. Soc., Dalt. Trans.* **1999**, 1311–1317.
[21] D. L. Clark, D. E. Hobart, P. D. Palmer, J. C. Sullivan, B. E. Stout, *J. Alloys Compd.* **1993**, *193*, 94–97.
[22] E. Brucher, J. Glaser, I. Toth, *Inorg. Chem.* **1991**, *30*, 2239–2241.
[23] A. F. Panasci, S. J. Harley, M. Zavarin, W. H. Casey, *Inorg. Chem.* **2014**, *53*, 4202–4208.
[24] C. D. Pilgrim, M. Zavarin, W. H. Casey, *Inorg. Chem.* **2017**, *56*, 661–666.
[25] L. Rao, G. Tian, *Symmetry (Basel).* **2010**, *2*, 1–14.
[26] T. J. Swift, R. E. Connick, *J. Chem. Phys.* **1962**, *37*, 307.
[27] W. H. Casey, S. J. Harley, C. A. Olin, *Geochim. Cosmochim. Ac.* **2011**, *75*, 3711–3725.
[28] N. Bloembergen, E. M. Purcell, R. V. Pound, *Phys. Rev.* **1948**, *73*, 679–712.
[29] H. Eyring, *J. Chem. Phys.* **1934**, *3*, 107–115.
[30] M. G. Evans, M. Polanyi, *Trans. Faraday Soc.* **1935**, *31*, 875–894.

[31] P. G. Allen, J. J. Bucher, D. K. Shuh, N. M. Edelstein, T. Reich, *Inorg. Chem.* **1997**, *36*, 4676–4683.
[32] P. G. Allen, J. J. Bucher, D. L. Clark, N. M. Edelstein, S. A. Ekberg, J. W. Gohdes, E. A. Hudson, N. Kaltsoyannis, W. W. Lukens, M. P. Neu, et al., *Inorg. Chem.* **1995**, *34*, 4797–4807.
[33] C. Hennig, A. Ikeda-Ohno, S. Tsushima, A. C. Scheinost, *Inorg. Chem.* **2009**, *48*, 5350–5360.
[34] H. Stöber, *Mischkomplexe Und Höhere Uniligandenkomplexe Des Fünfwertigen Neptuniums- Zur Koordinationsfähigkeit Des NpO^{2+}-Ions*, Karlsruhe, **1972**.
[35] D. W. Boykin, *^{17}O NMR Spectroscopy in Organic Chemistry*, CRC Press, **1990**.
[36] C. A. Bunton, J. H. Carter, D. R. Llewellyn, C. O'Connor, A. L. Odell, S. Y. Yih, *J. Chem. Soc.* **1964**, 4615–4622.
[37] C. W. Davies, *Ion Association*, Butterworths, Washington, DC, **1962**.
[38] Gustafsson, J. P. *Visual MINTEQ*. Ver 3.1. Web. 26 Dec. 2017. <https://vminteq.lwr.kth.se/>.

Entry for the Table of Contents

FULL PAPER

The kinetics of the self-exchange reaction of oxalate around the NpO_2^+ metal center is studied using one-dimensional NMR with both ^{13}C and ^{17}O-labeled oxalate through near neutral to alkaline conditions.

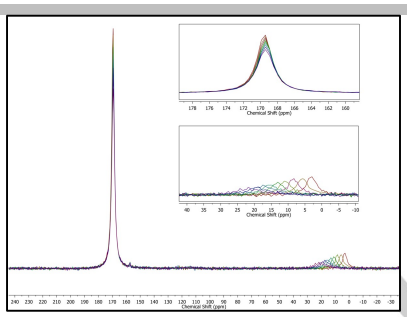

*C.D. Pilgrim, H.E. Mason, M. Zavarin, and W.H. Casey**

Page No. – Page No.

Rates of ligand exchange around the bis-oxalato complex $NpO_2(C_2O_4)_2^{3-}$ measured using multinuclear NMR at neutral to semi-alkaline conditions